energies

MDPI

Article

Study of Bulk Properties Relation to SARA Composition Data of Various Vacuum Residues Employing Intercriteria Analysis

Dicho Stratiev [1,2,*], Ivelina Shishkova [1], Georgi Nikolov Palichev [2], Krassimir Atanassov [2], Simeon Ribagin [2,3], Svetoslav Nenov [4], Dimitar Nedanovski [5] and Vitaly Ivanov [3]

1 LUKOIL Neftohim Burgas, 8104 Burgas, Bulgaria
2 Institute of Biophysics and Biomedical Engineering, Bulgarian Academy of Sciences, Academic Georgi Bonchev 105, 1113 Sofia, Bulgaria
3 Department Industrial Technologies and Management, University Prof. Dr. Assen Zlatarov, Professor Yakimov 1, 8010 Burgas, Bulgaria
4 Department of Mathematics, University of Chemical Technology and Metallurgy, Kliment Ohridski 8, 1756 Sofia, Bulgaria
5 Department of Mathematics, "St. Kliment Ohridski" University, 15 Tsar Osvoboditel Blvd., 1504 Sofia, Bulgaria
* Correspondence: stratiev.dicho@neftochim.bg

Abstract: Twenty-two straight run vacuum residues extracted from extra light, light, medium, heavy, and extra heavy crude oils and nine different hydrocracked vacuum residues were characterized for their bulk properties and SARA composition using four and eight fractions (SAR-AD^{TM}) methods. Intercriteria analysis was employed to determine the statistically meaningful relations between the SARA composition data and the bulk properties. The determined strong relations were modeled using the computer algebra system Maple and NLPSolve with the Modified Newton Iterative Method. It was found that the SAR-AD^{TM} saturates, and the sum of the contents of saturates and ARO-1 can be predicted from vacuum residue density, while the SAR-AD^{TM} asphaltene fraction content, and the sum of asphaltenes, and resins contents correlate with the softening point of the straight run vacuum residues. The softening point of hydrocracked vacuum residues was found to strongly negatively correlates with SAR-AD^{TM} Aro-1 fraction, and strongly positively correlates with SAR-AD^{TM} Aro-3 fraction. While in the straight run vacuum residues, the softening point is controlled by the content of SAR-AD^{TM} asphaltene fraction in the H-Oil hydrocracked vacuum residues, the softening point is controlled by the content of SAR-AD^{TM} Aro-3 fraction content. During high severity H-Oil operation, resulting in higher conversion, hydrocracked vacuum residue with higher SAR-AD^{TM} Aro-3 fraction content is obtained, which makes it harder and more brittle.

Keywords: vacuum residue; hydrocracked vacuum residue; intercriteria analysis; SARA; SAR-AD^{TM}; modeling; bulk properties; softening point

Citation: Stratiev, D.; Shishkova, I.; Palichev, G.N.; Atanassov, K.; Ribagin, S.; Nenov, S.; Nedanovski, D.; Ivanov, V. Study of Bulk Properties Relation to SARA Composition Data of Various Vacuum Residues Employing Intercriteria Analysis. *Energies* **2022**, *15*, 9042. https://doi.org/10.3390/en15239042

Academic Editor: Vladimir Alvarado

Received: 13 October 2022
Accepted: 25 November 2022
Published: 29 November 2022

1. Introduction

The vacuum residue is the heaviest petroleum fraction, which is the most difficult to characterize because of its low volatility, and the myriad components it contains [1]. The number of components building a petroleum vacuum residue is still unknown, suggesting that it may be equal to or higher than 10^6 [1–3]. The distillation fractionation employed to separate petroleum to reduce its composition complexity is inapplicable for vacuum residues because of their low volatility. Since its introduction in the 1960s, SARA (Saturates, Aromatics, Resins, Asphaltenes) fractionation [4] has found a wide application for the characterization of vacuum residues and for the assessment of the effect of SARA composition on the performance of different refining processes [5–13]. Various SARA fractionation methods have been developed and used for the characterization of vacuum residues of different origins [14–26]. As a whole, SARA analysis methods can be divided into three main groups: liquid chromatography, thin layer chromatography/flame ionization detection (TLC/FID), and high performance liquid chromatography (HPLC) [27]. They can also be classified as four and eight SARA fraction methodologies [28]. The SARA composition data can be used for evaluating relations between different SARA fractions [29], assessing the quality of petroleum [30], judging oil fouling potential [10], estimating vacuum residue properties [31], and understanding the chemical transformations taking place in vacuum residue upgrading processes [32,33]. Different approaches have been reported to predict the SARA composition of petroleum from other petroleum characteristics [34–37]. The presence of correlations of bulk properties to SARA composition data can allow prediction of SARA fraction contents, and vice versa prediction of bulk properties from SARA composition data. Our earlier studies employed the more traditional four fraction SARA method to investigate the relations between vacuum residue SARA composition data and vacuum residue bulk properties [37–39]. In this study, we availed the more sophisticated SARA separations into eight fractions of twenty-five straight run vacuum residues derived from extra light, light, medium, heavy, and extra heavy crude oils, and nine different hydrocracked vacuum residues by application of SAR-AD^{TM} method, developed by the Western Research Institute [25]. Besides the eight SARA fraction compositions, the vacuum residue bulk properties, namely density, Conradson carbon content, viscosity, softening point, and sulfur content, of the thirty-four vacuum residues were also measured. The thirty-four vacuum residues were also analyzed by the more traditional four fraction SARA method, developed in the research laboratory of LUKOIL Neftohim Burgas [24]. Eleven of the thirty-four studied in this work vacuum residues were also analyzed by the four fraction SARA method following the standard ASTM D4124. Some of the vacuum residues were analyzed for their four fraction SARA composition following the procedure IFP 9305. The relations between the SARA composition data and the bulk properties were evaluated by the use of intercriteria analysis (ICrA), as described in our recent research [40].

The aim of this study is to investigate the relationship of SARA fraction composition data to the vacuum residue bulk properties employing ICrA and using both four and eight fractions of SARA separations and to develop correlations for the established statistically meaningful relations.

2. Materials and Methods

Nineteen individual crude oils pertaining to the groups of extra light (specific gravity (SG) < 0.8017), light (0.8017 < SG < 0.855), medium (0.8600 < SG < 0.9220), heavy (0.9220 < SG < 1.000), and extra-heavy (SG > 1.000) and three crude oil blends were characterized for their bulk density (ASTM D 4052 [41]), and sulfur content (ASTM D 4294 [42]). Then, they were fractionated in a TBP apparatus operating under the requirements of ASTM D 2892 [43] for the atmospheric part, and ASTM D 5236 for the vacuum part. The vacuum residue fractions (boiling above 540 °C) were characterized for their SARA composition according to the methodology developed in the LUKOIL Neftohim Burgas (LNB) Research Laboratory [24], and five of the straight run vacuum residues were characterized in accordance with the requirements of the standard ASTM D 4124 [19], and two of them were characterized for SARA composition following the procedure IFP 9305 [44]. Nine hydrocracked vacuum residues (VTB = vacuum tower bottom) obtained from the commercial LNB H-Oil ebullated bed vacuum residue hydrocracker at a vacuum residue conversion variation between 55% and 91% were characterized for their SARA composition following the procedure of the LNB Research Laboratory [24]. Six of them were characterized for SARA composition in accordance with the standard ASTM D 4124 [19], and two VTBs were characterized for SARA composition in accordance with the IFP 9305 procedure [44]. All thirty-four vacuum residues studied in this work were characterized for their eight fraction SARA (SAR-AD^{TM}) composition in accordance with the procedure described in [25,45]. In the SAR-AD fractionation, five distinct maltenes fractions (Saturates, Aro-1, Aro-2, Aro-3, Resins) are derived by chromatography, and three different asphaltene subfractions are gained by solubility using three different solvents of increasing solvent power: cyclohexane, toluene, and dichloromethane [46]. More details about SAR-AD^{TM} application to characterize straight run vacuum residues and hydrocracked H-Oil vacuum residues the reader can find in our recent study [47].

The softening point (Ring & Ball) of the thirty-four studied vacuum residues was measured according to BDS (Bulgarian standard) EN 1426.

The viscosity of blends of the twenty-two straight run vacuum residues with fluid catalytic cracking heavy cycle oil in a ratio of 70% VR/30% FCC HCO was measured according to ASTM D1665 (Engler specific viscosity of tar products) at 80 °C. The properties of the FCC HCO were as follows: density at 15 °C = 1.000 g/cm^3; HTSD (high temperature simulated distillation, ASTM D7169): (Evaporate, % = boiling point, °C) IBP = 241 °C; 10wt.% = 272 °C; 30wt.% = 297 °C; 50 wt.% = 316 °C; 70 wt.% = 337 °C; 90 wt.% = 367 °C; 95 wt.% = 382; FBP = 431 °C, kin. viscosity at 80 °C = 3.25 mm^2/s.

Conversion of Engler-specific viscosity in kinematic viscosity was performed following Equation (1) [48]:

$$\text{Kin. vis.} = 7.41\text{Engler specific viscosity} \quad (1)$$

where Kin. vis. = kinematic viscosity, mm^2/s. Engler specific viscosity = Engler specific viscosity, °E.

3. Results

Table 1 summarizes the results of measurements of crude oil density at 15 °C, sulfur content, vacuum residue fraction (>540 °C) TBP yield, crude oil $T_{50\%}$, vacuum residue density at 15 °C, Conradson carbon content (CCR), and sulfur content, four fractions SARA composition data according to the procedure of the LNB Research laboratory [25], and eight fractions SARA (SAR-AD^{TM}) composition data according to the procedure of WRI [42–44]. Tables 2 and 3 present data of SARA composition of five straight run vacuum residues (Table 2), and six hydrocracked H-Oil vacuum residues (VTBs) (Table 3) measured by four different SARA methods: ASTM D4124, WRI SAR-AD^{TM}, IFP 9305, and LNB. Table 4 summarizes the data of H-Oil operating conditions, bulk properties, LNB four fractions SARA, and WRI eight fractions SAR-AD^{TM} composition data of hydrocracked vacuum residues (VTBs). Table 5 presents data for comparison of measured against estimated SAR-AD^{TM} fraction contents of blended vacuum residues using the linear additive rule. Table 6 presents data of μ-value of the ICrA evaluation of relations between crude oil and vacuum residue bulk properties, LNB SARA, and SAR-AD characteristics. Table 7 summarizes the data of υ-value of the ICrA evaluation of relations between crude oil and vacuum residue bulk properties, LNB SARA, and SAR-AD characteristics. Table 8 exhibits data of μ-value of the ICrA evaluation of relations between bulk properties, LNB SARA, SAR-AD characteristics of H-Oil VTB, and reaction severity. Table 9 presents data of υ-value of the ICrA evaluation of relations between bulk properties, LNB SARA, SAR-AD characteristics of H-Oil VTB, and reaction severity. An explanation of the ICrA approach is given in our recent study [41]. The meaning of $\mu = 0.75 \div 1.00$; $\upsilon = 0 \div 0.25$ denotes a statistically meaningful significant positive relation, where the strong positive consonance exhibits values of $\mu = 0.95 \div 1.00$; $\upsilon = 0 \div 0.05$, and the weak positive consonance exhibits values of $\mu = 0.75 \div 0.85$; $\upsilon = 0.15 \div 0.25$. Respectively, the values of negative consonance with $\mu = 0 \div 0.25$; $\upsilon = 0.75 \div 1.00$ means a statistically meaningful negative relation, where the strong negative consonance exhibits values of $\mu = 0 \div 0.05$; $\upsilon = 0.95 \div 1.00$, and the weak negative consonance exhibits values of $\mu = 0.15 \div 0.25$; $\upsilon = 0.75 \div 0.85$. All other cases are considered dissonance.

Table 1. Bulk properties of studied crude oils and derived thereof vacuum residue fractions and four and eight fractions SARA composition data of the vacuum residues.

Nr	Crude Oils	Crude D15	Crude S	>540	Crude T50	VR D15	VR CCR	VR S	VR Sat	VR Aro	VR Res.	VR C7asp	VR C5asp	VR KV	VR SP	Sat	Aro 1	Aro 2	Aro 3	Resins	CyC6	Toluene	CH_2Cl_2	Total Asp
1	Urals 1	0.877	1.53	25.2	378	0.997	17.5	3	25.6	52.5	7.8	14.1	17.6	220.9	40.1	18.2	7.0	20.7	33.0	14.0	2.4	4.4	0.1	6.9
2	Urals 2	0.875	1.39	24.94	377	0.995	17.2	2.9	22.4	66.5	4.9	6.3	13.9	195	42.4	19.8	7.6	22.7	32.6	11.7	2.0	3.6	0.1	5.7
3	Arab Med.	0.872	2.48	25.2	376	1.031	20.7	5.4	11.8	68.3	5.3	14.6	25.5	338.3	44.7	9.2	8.0	25.4	37.5	11.0	2.4	6.1	0.3	8.8
4	Arab Heavy	0.889	2.91	32	429	1.04	23.6	5.8	12.4	61.9	4.4	21.3	32.9	374.6	51.2	6.2	6.8	23.5	36.7	13.6	3.3	9.5	0.3	13.2
5	Basrah L	0.878	2.85	28.3	392	1.052	23.8	5.9	12.3	64.8	4.9	18	27.7	368.9	50.3	7.9	6.4	22.7	38.3	14.4	2.8	7.2	0.3	10.3
6	Basrah H	0.905	3.86	33.8	418	1.071	28.9	7.1	12.3	54.1	5.8	27.7	37	731.9	68.6	7.4	6.5	23.9	38.9	13.4	3.0	6.6	0.3	9.9
7	Kirkuk	0.873	2.65	24.6	345	1.054	25.2	5.9	15.2	55.4	5	24.3	33.1	514.1	58.1	9.5	6.6	23.3	39.2	10.2	2.3	8.4	0.5	11.2
8	El Bouri	0.891	1.76	26.2	401	1.05	25.5	3.3	12	57.9	12.6	17.5	27.3	303	45	14.7	8.3	21.4	33.8	10.1	2.3	8.8	0.5	11.6
9	CPC	0.805	0.63	9.3	238	0.956	16	2.1	44.6	40.8	10.3	3.4	11	65	25.2	39.6	10.5	18.1	22.4	7.0	0.4	1.6	0.2	2.3
10	LSCO	0.854	0.57	18.7	352	0.993	14	1.6	25	61.1	6.1	7.8	15.5	149.1	28.9	21.2	9.4	19.4	32.2	13.4	1.3	2.9	0.1	4.4
11	Prinos	0.875	3.71	20.3	349	1.108	32.8	9.1	12.6	50.6	6.8	30	38.8	550	69.2	4.6	4.6	17.4	44.8	11.1	1.8	14.9	0.6	17.3
12	Boscan	1.002	5.5	63.1	571	1.078	27.8	6	15.1	44.5	5.3	35.2	41	1003	115	1.6	1.9	12.3	26.6	23.4	8.1	25.6	0.5	34.2
13	Varandey	0.85	0.63	14.9	362	0.99	15.1	1.7	33.5	47.6	11.3	7.6	13.5	103	43.8	31.1	7.1	15.8	27.9	13.1	1.6	3.2	0.2	5.0
14	Albania	1.001	5.64	48.2	531	1.094	31.4	8.7	10	52.9	6.3	37.7	49.7	680	92.2	1.2	2.0	17.5	41.5	12.9	5.5	18.7	0.6	24.8
15	Tempa rossa	0.94	5.35	37.6	428	1.12	34.3	9.3	2.2	48.4	12.6	36.8	46.8	759.5	100	0.8	2.1	18.3	44.2	10.9	4.5	18.4	0.7	23.5
16	Rhemoura	0.865	0.75	20.2	350	1.041	23.7	1.8	19.7	49.8	7.3	23.2	31.3	255	51.1	15.7	7.6	18.5	36.0	11.4	1.9	8.5	0.4	10.8
17	Arab Light	0.858	1.89	22.9	352	1.029	18.7	4.9	15.9	64.7	7.3	12.1	18.8	192	32.3	11.3	11.1	28.1	34.8	9.0	1.6	4.0	0.2	5.8
18	Azeri Light	0.848	0.2	14.8	321	0.967	9.5	0.5	40.2	50.1	8.4	1.4	5.4	77	30.2	34.9	6.9	15.7	30.7	10.7	0.2	0.7	0.1	1.1
19	Imported AR	0.878	1.5	25.5	380	1.029	19.2	3.28	17.5	60.7	8	13.7	21.8	215	40.5	8.0	7.3	26.4	39.3	12.1	2.1	4.7	0.2	6.9
20	Ur.1(80%)/Basr L (20%)	0.877	1.79	25.82	381	1.007	18.8	3.58	22.94	54.96	11.2	10.9	15.9	225	39.5	17.8	7.4	24.0	33.1	11.0	2.0	4.5	0.1	6.7
21	Ur.1(70%)/Basr L (30%)	0.878	1.93	26.13	382	1.012	19.4	3.87	21.61	56.19	9.7	12.5	20.5	230	39.8	15.9	7.6	24.6	34.4	10.9	2.1	4.3	0.1	6.6
22	14%Ur.36%LSCO/ 50%ME	0.869	1.78	23.40	361	1.023	20.7	3.82	17.71	59.65	9.43	13.2	21.2	222	42	14.0	7.1	25.2	37.6	9.4	2.1	4.6	0.1	6.9
	Min	0.805	0.20	9.30	238	0.956	9.5	0.50	2.20	40.80	4.40	1.4	5.4	65	25.2	0.8	1.9	12.3	22.4	7.0	0.2	0.7	0.1	1.1
	Max	1.002	5.64	63.10	571	1.12	34.3	9.30	44.60	68.30	12.60	37.7	49.7	1003	115	39.6	11.1	28.1	44.8	23.4	8.1	25.6	0.7	34.2

Table 2. SARA composition data of straight run vacuum residues measured by ASTM D4124, SAR-AD^{TM}, IFP 9305, and LNB Research Laboratory methods.

ASTM D4124				WRI SAR-AD				IFP 9305				LNB			
Sat. wt.%	**Arom. wt.%**	**Resins. wt.%**	**Asphaltenes, wt.%**	**Sat. wt.%**	**Arom. wt.%**	**Resins, wt.%**	**Asphaltenes, wt.%**	**Sat. wt.%**	**Arom. wt.%**	**Resins, wt.%**	**Asphaltenes, wt.%**	**Sat. wt.%**	**Arom. wt.%**	**Resins, wt.%**	**Asphaltenes, wt.%**
14.0	36.2	43	6.8	19.8	62.9	11.7	5.7					25.6	52.5	7.8	14.1
17.1	38.6	35.9	7.2	18.2	60.8	14.0	6.9	17.5	39.5	35.7	5.8	22.4	66.5	4.9	6.3
13.3	39.9	40.3	6.5	17.8	64.5	11.0	6.7					22.9	55.0	11.2	10.9
11.7	36.8	43.7	7.8	15.9	66.6	10.9	6.6	12.0	36.7	40.5	8.0	21.6	56.2	9.7	12.5
10.1	39.1	42.7	8.1	14.0	69.8	9.4	6.9					17.7	59.6	9.4	13.2

Table 3. SARA composition data of H-Oil VTBs measured by ASTM D4124 method, SAR-AD^{TM} method, IFP 9305, and LNB Research Laboratory method.

ASTM D4124				WRI SAR-AD				IFP 9305				LNB			
Sat. wt.%	**Arom. wt.%**	**Resins. wt.%**	**Asphaltenes, wt.%**	**Sat. wt.%**	**Arom. wt.%**	**Resins, wt.%**	**Asphaltenes, wt.%**	**Sat. wt.%**	**Arom. wt.%**	**Resins, wt.%**	**Asphaltenes, wt.%**	**Sat. wt.%**	**Arom. wt.%**	**Resins, wt.%**	**Asphaltenes, wt.%**
17.8	40.6	35.6	6	27.44	61.5	6.03	5.68	27.2	36.0	28.0	5.0	34.5	41.0	8.8	15.7
17.1	38.6	35.9	8.4	26.98	60.2	5.93	6.95	24.9	33.9	30.1	8.9	29.1	53.9	5.0	12.0
15.9	37.6	35.1	11.4	21.01	66.8	5.97	6.24					19.4	54.6	4.7	21.3
16.4	38.9	35.1	9.6	21.96	65.7	6.19	6.7					23.5	54.8	6.9	14.8
15.7	36.6	37	10.7	19.76	68.2	6.01	6.58	18.4	33.4	35.5	9.7	22.6	48.9	10.0	18.5
15.2	40.8	34.4	9.6	19.72	71.1	4.37	6.85					21.5	52.6	8.6	17.3

Table 4. H-Oil operating conditions, bulk properties, LNB four fraction SARA, and WRI eight fraction SAR-AD^{TM} composition data of hydrocracked vacuum residues (VTBs).

Parameter	Case 1	Case 2	Case 3	Case 4	Case 5	Case 6	Case 7	Case 8	Case 9
Crude blend, processed in LNB refinery	100% Urals	100% Urals	85% Ur./ 15% ME	80% Ur./ 20% ME	70% Ur./ 30% ME	14% Ur./ 36% LSCO/ 50% ME	61.5% Ur/. 3% BL/2% AM/ 19.5% Kirkuk/ 7.5% LSCO/ 6.5% Prinos	64% Ur./25% Kirkuk/ 11% BL	88.6% Ur./5% LSCO/ 6.5% Kirkuk
FCC SLO in H-Oil feed, wt%	0.0	0.0	7.6	6.1	8.2	7.5	11.8	0.0	0.0
Recycle from H-Oil VTB, wt.%	0.0	0.0	0.0	0.0	0.0	0.0	29.4	12.89	0
WABT, °C	409	418	426	425	428	426	430.5	429.5	414.50
LHSV, h^{-1}	0.23	0.25	0.21	0.20	0.20	0.17	0.10	0.155	0.139
ATB TSE, wt.%	0.3	2.2	0.4	0.4	0.25	0.04	0.11	0.56	0.46
Conversion, wt.%	55	65	71.6	73	74.5	76.3	90.8	78.0	62.000
VTB D15, g/cm^3	0.985	1.005	1.029	1.033	1.041	1.034	1.102	1.066	1.0182
VTB CCR, wt.%	17.9	20.4	24.4	26	25.5	25.8	38	38.0	22.4
VTB Sulphur, wt.%	1.1	1.3	1.38	1.24	1.4	1.3	1.3	1.9	1.3
VTB LNB Saturates, wt.%	34.5	29.1	19.4	23.5	22.6	21.5	16.1	12.0	24.7
VTB LNB Aromatics, wt.%	41.0	53.9	54.6	54.8	48.9	52.6	39.8	57.5	49.0
VTB LNB Resins, wt.%	8.8	5.0	4.7	6.9	10.0	8.6	12.7	0.7	7.7
VTB LNB C_7 asphaltenes, wt.%	15.7	12	21.3	14.8	18.5	17.3	31.4	29.8	18.6
VTB LNB C_5 asphaltenes, wt.%	24.5	17	26.0	21.7	28.5	25.9	44.1	30.5	26.24
VTB softening point, °C	27.2	33	40	41.8	44.6	42	76	45.7	34.9
VTB Fraas breaking point, °C	−15	−14	−12	−10	−11	−9	25	−10	−14
VTB specifc Engler viscosity, °E	12.8	29.8	52.7	14.1	36.2	15.9	130.8	45.9	15.7
VTB SARA-AD^{TM} Saturates, wt.%	27.44	26.98	21.01	21.96	19.76	19.72	13.85	18.66	21.48
VTB SARA-AD^{TM} Aro 1, wt.%	9.34	8.22	6.85	7.15	6.77	7.48	3.04	5.92	8.41
VTB SARA-AD^{TM} Aro 2, wt.%	18.76	17.43	16.89	17.82	17.35	18.80	14.75	18.07	20.30
VTB SARA-AD^{TM} Aro 3, wt.%	33.41	34.59	43.04	40.77	44.09	44.86	60.20	44.74	39.67
VTB SARA-AD^{TM} Resins, wt.%	6.03	5.93	5.97	6.19	6.01	4.37	2.46	4.42	4.17
VTB SARA-AD^{TM} CyC6 asp, wt.%	0.38	0.34	0.23	0.25	0.23	0.17	0.07	0.22	0.14
VTB SARA-AD^{TM} Toluene asp.	4.47	6.12	5.56	5.47	5.47	4.28	4.90	7.00	5.28
VTB SARA-AD^{TM} CH_2Cl_2 asp., wt.%	0.18	0.39	0.46	0.39	0.33	0.32	0.71	0.95	0.53
VTB SARA-AD^{TM} Total asp, wt.%	5.03	6.85	6.24	6.11	6.03	4.77	5.68	8.17	5.95

Table 5. Comparison of measured and estimated SAR-AD™ fraction contents using the linear additive rule.

SRVR Blends	Sat	Aro 1	Aro 2	Aro 3	Resins	CyC6	Toluene	CH_2Cl_2	Total Asphaltenes
100% Urals	18.24	7.04	20.75	33.04	13.98	2.43	4.43	0.09	6.95
100% Basrah light	7.92	6.44	22.66	38.30	14.41	2.81	7.18	0.28	10.27
#33 H-Oil VTB from 80% Urals/20% Basrah light	17.79	7.42	23.97	33.10	11.03	2.04	4.55	0.09	6.68
Estimated assuming additivity (80% Ur./20% BL)	16.17	6.92	21.13	34.10	14.07	2.51	4.98	0.12	7.61
#27 70% Urals/30% Basrah Light	15.90	7.60	24.58	34.39	10.95	2.14	4.33	0.11	6.58
Estimated assuming additivity (70% Ur./30% BL)	15.14	6.86	21.32	34.62	14.11	2.55	5.26	0.14	7.95
#29 50% Urals/50% Basrah Light	14.0	7.1	25.2	37.6	9.4	2.1	4.6	0.1	6.9
Estimated assuming additivity (50% Ur./50% BL)	13.08	6.74	21.70	35.67	14.19	2.62	5.81	0.18	8.61

Table 6. μ-Value of the ICrA evaluation of relations between crude oil and vacuum residue bulk properties, LNB SARA, and SAR-AD characteristics.

μ	Crude D15	Crude S	>540	VR D15	VR CCR	VR S	VR Sat	VR Aro	VR Res.	VR C7asp	VR C5asp	VR VIS	VR SP	Sat	Aro 1	Aro 2	Aro 3	Resins	CyC6	Toluene	CH_2Cl_2	Total Asp
Crude D15	1.00	0.80	0.93	0.78	0.77	0.75	0.21	0.49	0.42	0.78	0.79	0.82	0.76	0.18	0.26	0.49	0.68	0.64	0.85	0.79	0.59	0.79
Crude S	0.80	1.00	0.82	0.85	0.85	0.94	0.18	0.49	0.37	0.84	0.86	0.89	0.79	0.11	0.24	0.53	0.75	0.57	0.82	0.83	0.67	0.83
>540	0.93	0.82	1.00	0.77	0.76	0.77	0.23	0.54	0.43	0.77	0.78	0.83	0.75	0.19	0.29	0.53	0.67	0.63	0.88	0.78	0.56	0.77
VR D15	0.78	0.85	0.77	1.00	0.94	0.88	0.13	0.48	0.39	0.92	0.94	0.90	0.86	0.08	0.26	0.49	0.82	0.55	0.77	0.88	0.77	0.87
VR CCR	0.77	0.85	0.76	0.94	1.00	0.89	0.16	0.44	0.44	0.90	0.91	0.89	0.85	0.13	0.27	0.46	0.79	0.53	0.77	0.89	0.75	0.88
VR S	0.75	0.94	0.77	0.88	0.89	1.00	0.17	0.49	0.41	0.83	0.85	0.86	0.78	0.11	0.26	0.54	0.80	0.52	0.77	0.81	0.68	0.80
VR Sat	0.21	0.18	0.23	0.13	0.16	0.17	1.00	0.40	0.61	0.19	0.17	0.18	0.23	0.87	0.64	0.42	0.21	0.46	0.20	0.19	0.15	0.19
VR Aro	0.49	0.49	0.54	0.48	0.44	0.49	0.40	1.00	0.32	0.43	0.45	0.45	0.42	0.47	0.63	0.78	0.58	0.48	0.51	0.45	0.33	0.44
VR Res.	0.42	0.37	0.43	0.39	0.44	0.41	0.61	0.32	1.00	0.39	0.39	0.38	0.39	0.62	0.57	0.45	0.43	0.30	0.37	0.40	0.36	0.38
VR C7asp	0.78	0.84	0.77	0.92	0.90	0.83	0.19	0.43	0.39	1.00	0.97	0.90	0.90	0.12	0.23	0.45	0.78	0.61	0.81	0.91	0.74	0.91
VR C5asp	0.79	0.86	0.78	0.94	0.91	0.85	0.17	0.45	0.39	0.97	1.00	0.91	0.90	0.10	0.24	0.48	0.81	0.59	0.80	0.92	0.74	0.91
VR VIS	0.82	0.89	0.83	0.90	0.89	0.86	0.18	0.45	0.38	0.90	0.91	1.00	0.88	0.12	0.24	0.47	0.77	0.61	0.83	0.89	0.68	0.88
VR SP	0.76	0.79	0.75	0.86	0.85	0.78	0.23	0.42	0.39	0.90	0.90	0.88	1.00	0.17	0.20	0.40	0.73	0.62	0.78	0.87	0.74	0.87
Sat	0.18	0.11	0.19	0.08	0.13	0.11	0.87	0.47	0.62	0.12	0.10	0.12	0.17	1.00	0.73	0.45	0.16	0.40	0.17	0.13	0.15	0.13
Aro 1	0.26	0.24	0.29	0.26	0.27	0.26	0.64	0.63	0.57	0.23	0.24	0.24	0.20	0.73	1.00	0.64	0.32	0.30	0.23	0.25	0.24	0.23
Aro 2	0.49	0.53	0.53	0.49	0.46	0.54	0.42	0.78	0.45	0.45	0.48	0.47	0.40	0.45	0.64	1.00	0.61	0.41	0.51	0.43	0.31	0.42
Aro 3	0.68	0.75	0.67	0.82	0.79	0.80	0.21	0.58	0.43	0.78	0.81	0.77	0.73	0.16	0.32	0.61	1.00	0.48	0.66	0.75	0.61	0.74
Resins	0.64	0.57	0.63	0.55	0.53	0.52	0.46	0.48	0.30	0.61	0.59	0.61	0.62	0.40	0.30	0.41	0.48	1.00	0.63	0.59	0.44	0.59
CyC6	0.85	0.82	0.88	0.77	0.77	0.77	0.20	0.51	0.37	0.81	0.80	0.83	0.78	0.17	0.23	0.51	0.66	0.63	1.00	0.81	0.61	0.82
Toluene	0.79	0.83	0.78	0.88	0.89	0.81	0.19	0.45	0.40	0.91	0.92	0.89	0.87	0.13	0.25	0.43	0.75	0.59	0.81	1.00	0.74	0.98
CH_2Cl_2	0.59	0.67	0.56	0.77	0.75	0.68	0.15	0.33	0.36	0.74	0.74	0.68	0.74	0.15	0.24	0.31	0.61	0.44	0.61	0.74	1.00	0.74
Total Asp	0.79	0.83	0.77	0.87	0.88	0.80	0.19	0.44	0.38	0.91	0.91	0.88	0.87	0.13	0.23	0.42	0.74	0.59	0.82	0.98	0.74	1.00

Note: Green color means statistically meaningful positive relation; Red color implies statistically meaningful negative relation. The intensity of the color designates the strength of the relation. The higher the color intensity, the higher the strength of the relation is. Yellow color denotes dissonance.

Table 7. υ-Value of the ICrA evaluation of relations between crude oil and vacuum residue bulk properties, LNB SARA, and SAR-AD characteristics.

υ	Crude D15	Crude S	>540	VR D15	VR CCR	VR S	VR Sat	VR Aro	VR Res.	VR C7asp	VR C5asp	VR VIS	VR SP	Sat	Aro 1	Aro 2	Aro 3	Resins	CyC6	Toluene	CH_2Cl_2	Total Asp
Crude D15	0.000	0.173	0.043	0.195	0.199	0.221	0.762	0.489	0.541	0.195	0.186	0.156	0.221	0.797	0.706	0.485	0.303	0.325	0.104	0.186	0.234	0.178
Crude S	0.173	0.000	0.173	0.143	0.143	0.052	0.810	0.507	0.606	0.152	0.134	0.104	0.204	0.887	0.740	0.463	0.242	0.411	0.143	0.165	0.178	0.156
>540	0.043	0.173	0.000	0.225	0.234	0.221	0.766	0.455	0.550	0.221	0.212	0.165	0.247	0.810	0.684	0.459	0.329	0.351	0.091	0.217	0.273	0.212
Crude T50	0.095	0.238	0.078	0.299	0.290	0.286	0.701	0.476	0.515	0.294	0.286	0.238	0.294	0.745	0.658	0.489	0.403	0.303	0.139	0.255	0.312	0.260
VR D15	0.195	0.143	0.225	0.000	0.052	0.108	0.866	0.520	0.584	0.074	0.056	0.095	0.134	0.913	0.714	0.498	0.173	0.429	0.199	0.113	0.078	0.113
VR CCR	0.199	0.143	0.234	0.052	0.000	0.104	0.836	0.558	0.537	0.100	0.082	0.104	0.143	0.862	0.710	0.528	0.204	0.455	0.195	0.104	0.087	0.100
VR S	0.221	0.052	0.221	0.108	0.104	0.000	0.823	0.502	0.571	0.169	0.143	0.139	0.212	0.883	0.719	0.450	0.199	0.459	0.191	0.191	0.152	0.186
VR Sat	0.762	0.810	0.766	0.866	0.836	0.823	0.000	0.597	0.368	0.801	0.827	0.814	0.766	0.126	0.338	0.567	0.788	0.524	0.766	0.810	0.693	0.797
VR Aro	0.489	0.507	0.455	0.520	0.558	0.502	0.597	0.000	0.667	0.571	0.546	0.550	0.580	0.533	0.355	0.217	0.420	0.502	0.463	0.550	0.507	0.550
VR Res.	0.541	0.606	0.550	0.584	0.537	0.571	0.368	0.667	0.000	0.597	0.597	0.602	0.589	0.364	0.394	0.537	0.554	0.667	0.584	0.584	0.459	0.589
VR C7asp	0.195	0.152	0.221	0.074	0.100	0.169	0.801	0.571	0.597	0.000	0.026	0.100	0.104	0.879	0.758	0.541	0.221	0.381	0.160	0.091	0.100	0.074
VR C5asp	0.186	0.134	0.212	0.056	0.082	0.143	0.827	0.546	0.597	0.026	0.000	0.091	0.104	0.905	0.740	0.515	0.195	0.398	0.169	0.082	0.100	0.074
VR VIS	0.156	0.104	0.165	0.095	0.104	0.139	0.814	0.550	0.602	0.100	0.091	0.000	0.117	0.883	0.745	0.528	0.225	0.377	0.143	0.113	0.156	0.104
VR SP	0.221	0.204	0.247	0.134	0.143	0.212	0.766	0.580	0.589	0.104	0.104	0.117	0.000	0.827	0.784	0.593	0.273	0.364	0.191	0.126	0.104	0.113
Sat	0.797	0.887	0.810	0.913	0.862	0.883	0.126	0.533	0.364	0.879	0.905	0.883	0.827	0.000	0.251	0.550	0.840	0.589	0.801	0.866	0.693	0.853
Aro 1	0.706	0.740	0.684	0.714	0.710	0.719	0.338	0.355	0.394	0.758	0.740	0.745	0.784	0.251	0.000	0.342	0.658	0.667	0.719	0.736	0.589	0.745
Aro 2	0.485	0.463	0.459	0.498	0.528	0.450	0.567	0.217	0.537	0.541	0.515	0.528	0.593	0.550	0.342	0.000	0.381	0.571	0.459	0.563	0.528	0.563
Aro 3	0.303	0.242	0.329	0.173	0.204	0.199	0.788	0.420	0.554	0.221	0.195	0.225	0.273	0.840	0.658	0.381	0.000	0.507	0.312	0.251	0.229	0.251
Resins	0.325	0.411	0.351	0.429	0.455	0.459	0.524	0.502	0.667	0.381	0.398	0.377	0.364	0.589	0.667	0.571	0.507	0.000	0.325	0.394	0.390	0.385
CyC6	0.104	0.143	0.091	0.199	0.195	0.191	0.766	0.463	0.584	0.160	0.169	0.143	0.191	0.801	0.719	0.459	0.312	0.325	0.000	0.160	0.234	0.143
Toluene	0.186	0.165	0.217	0.113	0.104	0.191	0.810	0.550	0.584	0.091	0.082	0.113	0.126	0.866	0.736	0.563	0.251	0.394	0.160	0.000	0.100	0.009
CH_2Cl_2	0.234	0.178	0.273	0.078	0.087	0.152	0.693	0.507	0.459	0.100	0.100	0.156	0.104	0.693	0.589	0.528	0.229	0.390	0.234	0.100	0.000	0.095
Total Asp	0.178	0.156	0.212	0.113	0.100	0.186	0.797	0.550	0.589	0.074	0.074	0.104	0.113	0.853	0.745	0.563	0.251	0.385	0.143	0.009	0.095	0.000

Note: Green color means statistically meaningful positive relation; Red color implies statistically meaningful negative relation. The intensity of the color designates the strength of the relation. The higher the color intensity, the higher the strength of the relation is. Yellow color denotes dissonance.

Table 8. µ-Value of the ICrA evaluation of relations between bulk properties, LNB SARA, SAR-AD characteristics of H-Oil VTB, and reaction severity.

µ	TRX	LHSV	Conv.	D15	CCR	Sul.	Sat. [1]	Aro [1]	Res. [1]	C7 Asp. [1]	C5 Asp. [1]	SP.	Fraas	VIS	Sat	Aro 1	Aro 2	Aro 3	Resins	CyC6	Toluene	CH_2Cl_2	Total Asp.
TRX	1.00	0.25	0.92	0.92	0.81	0.67	0.11	0.53	0.50	0.78	0.81	0.92	0.81	0.83	0.08	0.03	0.28	0.89	0.36	0.22	0.56	0.64	0.56
LHSV	0.25	1.00	0.19	0.19	0.19	0.31	0.69	0.53	0.39	0.19	0.17	0.19	0.19	0.36	0.81	0.67	0.42	0.22	0.75	0.86	0.64	0.28	0.61
Conv.	0.92	0.19	1.00	0.94	0.89	0.61	0.14	0.58	0.53	0.72	0.75	0.94	0.89	0.78	0.08	0.11	0.36	0.92	0.36	0.22	0.50	0.58	0.50
D15	0.92	0.19	0.94	1.00	0.89	0.64	0.14	0.53	0.58	0.78	0.81	1.00	0.86	0.78	0.08	0.11	0.36	0.92	0.36	0.22	0.50	0.64	0.50
CCR	0.81	0.19	0.89	0.89	1.00	0.56	0.14	0.61	0.47	0.67	0.69	0.89	0.86	0.67	0.11	0.14	0.39	0.86	0.39	0.25	0.50	0.67	0.53
Sul.	0.67	0.31	0.61	0.64	0.56	1.00	0.17	0.53	0.28	0.61	0.64	0.64	0.56	0.69	0.17	0.17	0.33	0.61	0.36	0.28	0.61	0.58	0.61
Sat. [1]	0.11	0.69	0.14	0.14	0.14	0.17	1.00	0.39	0.56	0.19	0.22	0.14	0.17	0.19	0.89	0.86	0.67	0.11	0.67	0.75	0.39	0.25	0.42
Aro [1]	0.53	0.53	0.58	0.53	0.61	0.53	0.39	1.00	0.11	0.47	0.39	0.53	0.53	0.53	0.50	0.42	0.56	0.50	0.61	0.56	0.72	0.61	0.75
Res. [1]	0.50	0.39	0.53	0.58	0.47	0.28	0.56	0.11	1.00	0.53	0.61	0.58	0.53	0.47	0.44	0.53	0.44	0.56	0.44	0.42	0.19	0.33	0.19
C7 asp. [1]	0.78	0.19	0.72	0.78	0.67	0.61	0.19	0.47	0.53	1.00	0.92	0.78	0.64	0.78	0.19	0.22	0.42	0.75	0.25	0.19	0.50	0.75	0.50
C5 asp. [1]	0.81	0.17	0.75	0.81	0.69	0.64	0.22	0.39	0.61	0.92	1.00	0.81	0.67	0.75	0.17	0.19	0.44	0.78	0.28	0.19	0.47	0.72	0.47
SP.	0.92	0.19	0.94	1.00	0.89	0.64	0.14	0.53	0.58	0.78	0.81	1.00	0.86	0.78	0.08	0.11	0.36	0.92	0.36	0.22	0.50	0.64	0.50
Fraas	0.81	0.19	0.89	0.86	0.86	0.56	0.17	0.53	0.53	0.64	0.67	0.86	1.00	0.67	0.11	0.17	0.39	0.89	0.33	0.19	0.42	0.56	0.44
VIS	0.83	0.36	0.78	0.78	0.67	0.69	0.19	0.53	0.47	0.78	0.75	0.78	0.67	1.00	0.19	0.17	0.19	0.75	0.36	0.31	0.61	0.72	0.61
Sat	0.08	0.81	0.08	0.08	0.11	0.17	0.89	0.50	0.44	0.19	0.17	0.08	0.11	0.19	1.00	0.86	0.61	0.06	0.72	0.83	0.50	0.31	0.53
Aro 1	0.03	0.67	0.11	0.11	0.14	0.17	0.86	0.42	0.53	0.22	0.19	0.11	0.17	0.17	0.86	1.00	0.75	0.14	0.58	0.69	0.36	0.28	0.39
Aro 2	0.28	0.42	0.36	0.36	0.39	0.33	0.67	0.56	0.44	0.42	0.44	0.36	0.39	0.19	0.61	0.75	1.00	0.39	0.44	0.47	0.39	0.39	0.42
Aro 3	0.89	0.22	0.92	0.92	0.86	0.61	0.11	0.50	0.56	0.75	0.78	0.92	0.89	0.75	0.06	0.14	0.39	1.00	0.28	0.14	0.47	0.61	0.47
Resins	0.36	0.75	0.36	0.36	0.39	0.36	0.67	0.61	0.44	0.25	0.28	0.36	0.33	0.36	0.72	0.58	0.44	0.28	1.00	0.86	0.50	0.28	0.53
CyC6	0.22	0.86	0.22	0.22	0.25	0.28	0.75	0.56	0.42	0.19	0.19	0.22	0.19	0.31	0.83	0.69	0.47	0.14	0.86	1.00	0.56	0.25	0.58
Toluene	0.56	0.64	0.50	0.50	0.50	0.61	0.39	0.72	0.19	0.50	0.47	0.50	0.42	0.61	0.50	0.36	0.39	0.47	0.50	0.56	1.00	0.64	0.97
CH_2Cl_2	0.64	0.28	0.58	0.64	0.67	0.58	0.25	0.61	0.33	0.75	0.72	0.64	0.56	0.72	0.31	0.28	0.39	0.61	0.28	0.25	0.64	1.00	0.67
Total asp.	0.56	0.61	0.50	0.50	0.53	0.61	0.42	0.75	0.19	0.50	0.47	0.50	0.44	0.61	0.53	0.39	0.42	0.47	0.53	0.58	0.97	0.67	1.00

Note: Green color means statistically meaningful positive relation; Red color implies statistically meaningful negative relation. The intensity of the color designates the strength of the relation. The higher the color intensity, the higher the strength of the relation is. Yellow color denotes dissonance. [1] This denotes SARA composition performed in accordance with the procedure described in [25].

Table 9. υ-Value of the ICrA evaluation of relations between bulk properties, LNB SARA, SAR-AD characteristics of H-Oil VTB, and reaction severity.

υ	TRX	LHSV	Conv.	D15	CCR	Sul.	Sat. [1]	Aro [1]	Res. [1]	C7 Asp. [1]	C5 Asp. [1]	SP.	Fraas	VIS	Sat	Aro 1	Aro 2	Aro 3	Resins	CyC6	Toluene	CH_2Cl_2	Total Asp.
TRX	0.00	0.69	0.06	0.06	0.14	0.14	0.86	0.44	0.47	0.19	0.17	0.06	0.11	0.14	0.89	0.94	0.69	0.08	0.61	0.72	0.39	0.31	0.42
LHSV	0.69	0.00	0.78	0.78	0.75	0.50	0.28	0.44	0.58	0.78	0.81	0.78	0.72	0.61	0.17	0.31	0.56	0.75	0.22	0.08	0.36	0.67	0.36
Conv.	0.06	0.78	0.00	0.06	0.08	0.22	0.86	0.42	0.47	0.28	0.25	0.06	0.06	0.22	0.92	0.89	0.64	0.08	0.64	0.75	0.47	0.39	0.50
D15	0.06	0.78	0.06	0.00	0.08	0.19	0.86	0.47	0.42	0.22	0.19	0.00	0.08	0.22	0.92	0.89	0.64	0.08	0.64	0.75	0.47	0.33	0.50
CCR	0.14	0.75	0.08	0.08	0.00	0.25	0.83	0.36	0.50	0.31	0.28	0.08	0.06	0.31	0.86	0.83	0.58	0.11	0.58	0.69	0.44	0.28	0.44
Sul.	0.14	0.50	0.22	0.19	0.25	0.00	0.67	0.31	0.56	0.22	0.19	0.19	0.28	0.14	0.67	0.67	0.50	0.22	0.47	0.53	0.19	0.22	0.22
Sat.	0.86	0.28	0.86	0.86	0.83	0.67	0.00	0.61	0.44	0.81	0.78	0.86	0.78	0.81	0.11	0.14	0.33	0.89	0.33	0.22	0.58	0.72	0.58
Aro	0.44	0.44	0.42	0.47	0.36	0.31	0.61	0.00	0.89	0.53	0.61	0.47	0.42	0.47	0.50	0.58	0.44	0.50	0.39	0.42	0.25	0.36	0.25
Res.	0.47	0.58	0.47	0.42	0.50	0.56	0.44	0.89	0.00	0.47	0.39	0.42	0.42	0.53	0.56	0.47	0.56	0.44	0.56	0.56	0.78	0.64	0.81
C7 asp.	0.19	0.78	0.28	0.22	0.31	0.22	0.81	0.53	0.47	0.00	0.08	0.22	0.31	0.22	0.81	0.78	0.58	0.25	0.75	0.78	0.47	0.22	0.50
C5 asp.	0.17	0.81	0.25	0.19	0.28	0.19	0.78	0.61	0.39	0.08	0.00	0.19	0.28	0.25	0.83	0.81	0.56	0.22	0.72	0.78	0.50	0.25	0.53
SP.	0.06	0.78	0.06	0.00	0.08	0.19	0.86	0.47	0.42	0.22	0.19	0.00	0.08	0.22	0.92	0.89	0.64	0.08	0.64	0.75	0.47	0.33	0.50
Fraas	0.11	0.72	0.06	0.08	0.06	0.28	0.78	0.42	0.42	0.31	0.28	0.08	0.00	0.28	0.83	0.78	0.56	0.06	0.61	0.72	0.50	0.36	0.50
VIS	0.14	0.61	0.22	0.22	0.31	0.14	0.81	0.47	0.53	0.22	0.25	0.22	0.28	0.00	0.81	0.83	0.81	0.25	0.64	0.67	0.36	0.25	0.39
Sat	0.89	0.17	0.92	0.92	0.86	0.67	0.11	0.50	0.56	0.81	0.83	0.92	0.83	0.81	0.00	0.14	0.39	0.94	0.28	0.14	0.47	0.67	0.47
Aro 1	0.94	0.31	0.89	0.89	0.83	0.67	0.14	0.58	0.47	0.78	0.81	0.89	0.78	0.83	0.14	0.00	0.25	0.86	0.42	0.28	0.61	0.69	0.61
Aro 2	0.69	0.56	0.64	0.64	0.58	0.50	0.33	0.44	0.56	0.58	0.56	0.64	0.56	0.81	0.39	0.25	0.00	0.61	0.56	0.50	0.58	0.58	0.58
Aro 3	0.08	0.75	0.08	0.08	0.11	0.22	0.89	0.50	0.44	0.25	0.22	0.08	0.06	0.25	0.94	0.86	0.61	0.00	0.72	0.83	0.50	0.36	0.53
Resins	0.61	0.22	0.64	0.64	0.58	0.47	0.33	0.39	0.56	0.75	0.72	0.64	0.61	0.64	0.28	0.42	0.56	0.72	0.00	0.11	0.47	0.69	0.47
CyC6	0.72	0.08	0.75	0.75	0.69	0.53	0.22	0.42	0.56	0.78	0.78	0.75	0.72	0.67	0.14	0.28	0.50	0.83	0.11	0.00	0.39	0.69	0.39
Toluene	0.39	0.36	0.47	0.47	0.44	0.19	0.58	0.25	0.78	0.47	0.50	0.47	0.50	0.36	0.47	0.61	0.58	0.50	0.47	0.39	0.00	0.31	0.00
CH_2Cl_2	0.31	0.67	0.39	0.33	0.28	0.22	0.72	0.36	0.64	0.22	0.25	0.33	0.36	0.25	0.67	0.69	0.58	0.36	0.69	0.69	0.31	0.00	0.31
Total asp.	0.42	0.36	0.50	0.50	0.44	0.22	0.58	0.25	0.81	0.50	0.53	0.50	0.50	0.39	0.47	0.61	0.58	0.53	0.47	0.39	0.00	0.31	0.00

Note: Green color means statistically meaningful positive relation; Red color implies statistically meaningful negative relation. The intensity of the color designates the strength of the relation. The higher the color intensity, the higher the strength of the relation is. Yellow color denotes dissonance. [1] This denotes SARA composition performed in accordance with the procedure described in [25].

4. Discussion

The data in Table 1 indicate that the range of variation of all investigated properties is quite wide to allow representative investigation of the presence of statistically meaningful relations between crude oil and vacuum residue properties with SARA composition data.

The data in Tables 2 and 3 compare the SARA composition of the same straight run and hydrocracked vacuum residues measured by four different methods. These data confirm that different methodologies report distinct SARA compositions of the same vacuum residue samples. Therefore, the data gathered from different SARA methods cannot be used to search for the presence of statistically meaningful relations with the crude oil and vacuum residue bulk properties. For that reason, in this study we employed two SARA methods (the more traditional four fractions SARA method—that of the LNB research laboratory, and the eight fractions SAR-AD^{TM} method developed in WRI) to characterize all primary and secondary vacuum residues.

Similar to the data in Table 1, the data in Table 4 also indicates a relatively wide range of variation of properties of hydrocracked vacuum residue obtained from the LUKOIL Neftohim Burgas H-Oil vacuum residue hydrocracker. This wide range of property variation of the hydrocracked vacuum residues is mainly a result of the broad scope of alteration of H-Oil operating conditions and the resulting wide spread of conversion levels, between 55% and 91%.

Since the SARA fractions are solubility class components and, as such, during blending, a redistribution between the different fractions due to alteration of solubility of the original components may occur, we compared the contents of SAR-AD^{TM} eight fractions of vacuum residue blends with those calculated using the linear additive rule. The results of this comparison are shown in Table 5. One can see from this data that the difference between the measured and calculated eight SAR-AD^{TM} fractions contents (marked in red) is not substantial. Thus, it may be deduced that the SAR-AD^{TM} fractions may be considered pseudo-individual components that obey the additive rule.

The data in Tables 6–9 summarizes the ICrA evaluation results from the relations between the crude oil, and straight vacuum residue bulk properties, and hydrocracked vacuum residue bulk properties, and the four, and the eight fractions SARA composition data. To visualize the results in the ICrA evaluation, we use color scales, e.g., from green for the results of positive consonance, to red for the results of negative consonance, and yellow for dissonance. This colorization scheme allows for more immediate, human-friendly detection and interpretation of the results. It is evident from the data in Tables 6 and 7 that the SAR-AD^{TM} saturates content in the straight run vacuum residues (SRVR) has a strong statistically meaningful negative relation with density ($\mu = 0.08$; $\nu = 0.913$). The same observation is made for the SAR-AD^{TM} saturates content in the hydrocracked vacuum residue (H-Oil VTB) with the VTB density at 15 °C ($\mu = 0.08$; $\nu = 0.92$) from the data in Tables 8 and 9. By the use of the computer algebra system Maple and NLPSolve with Modified Newton Iterative Method, the following models, which relate density of SRVR and H-Oil VTB to densities, were developed (Equations (2) and (3))

$$\text{SRVR Sat} = -899.9999 - \frac{100}{-0.1115+1999.9999*\text{EXP}(-13.4596*D_{15})} \quad R = 0.95;$$
$$\text{av.dev.} = 2.4\ \text{wt.\%};\ \text{max. dev.} = 7.4\ \text{wt.\%};\ \text{bias} = 0.0\ \text{wt.\%} \qquad (2)$$

$$\text{HOil VTB Sat} = -20.7655 - \frac{100}{-9.5986+19.7397*\text{EXP}(-0.9792*D_{15})} \quad R = 0.96;$$
$$\text{av.dev.} = 0.85\ \text{wt.\%};\ \text{max. dev.} = 2.7\ \text{wt.\%};\ \text{bias} = -0.46\ \text{wt.\%} \qquad (3)$$

Figures 1 and 2 show graphs of the relation of density to saturates for both SRVRs, and H-Oil VTB using Equations (2) and (3) for SAR-AD^{TM} saturates, and for the LNB saturates the regression developed in our recent research [38] was used.

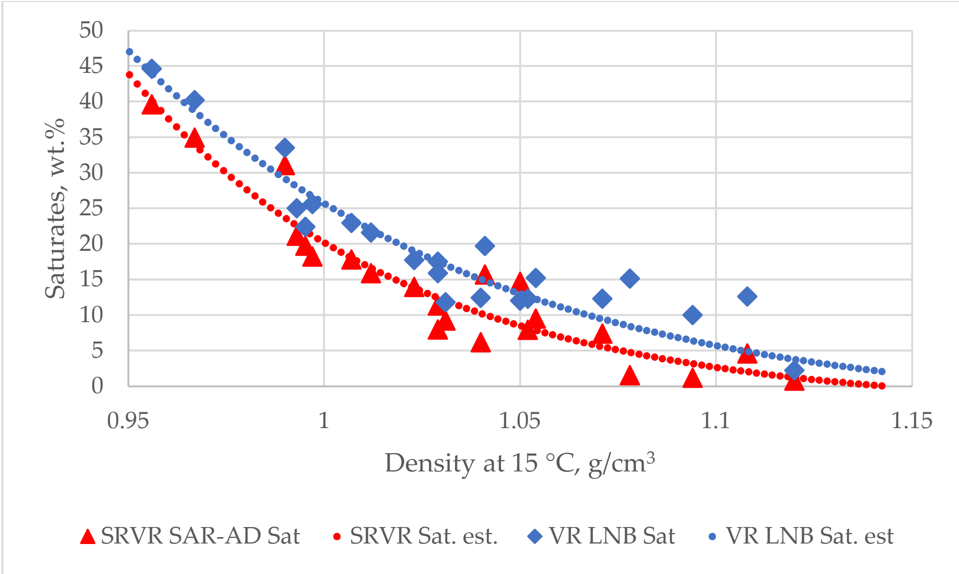

Figure 1. Relation of straight run vacuum residue density to saturate content determined by SAR-AD™ and LNB SARA methods.

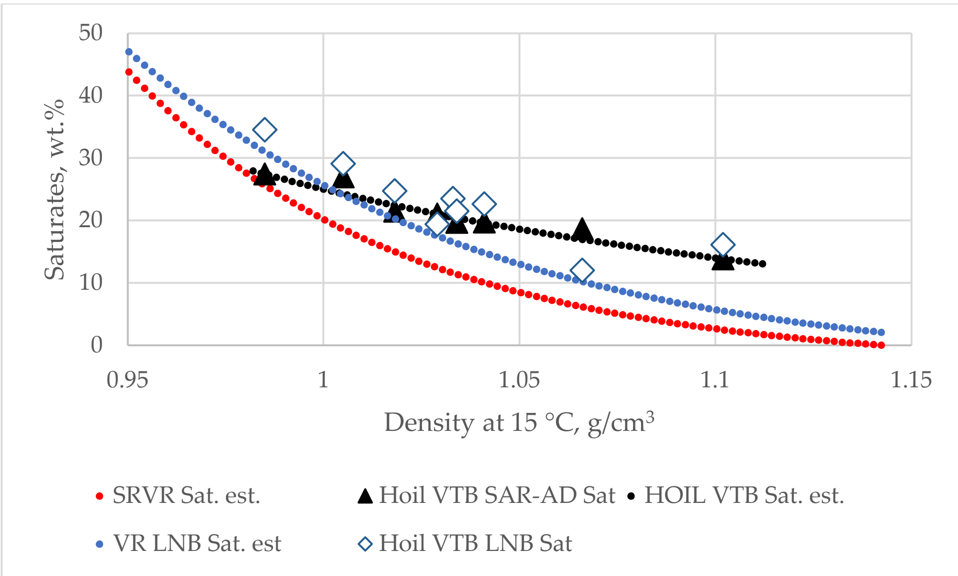

Figure 2. Relation of hydrocracked vacuum residue density to saturate content determined by SAR-AD™ and LNB SARA methods.

It is interesting to note here that the LNB SARA method reports a higher content of saturates than the SAR-AD™ method for SRVRs (Figure 1), while for the H-Oil VTBs, the contents of saturates are almost the same for both methods (Figure 2). It is also evident from the data in Figure 2 that the saturate content in H-Oil VTBs is higher than that in the SRVRs for both SARA methods. These findings suggest that the differences in the contents of SARA fractions reported by the various SARA methods can be diverse for distinct samples. If one takes a look at the data in Table 2, they can see almost the same figures for SARA composition of SRVRs reported by the methods ASTM D 4124, and IFP 9305. However, if the data in Table 3 are scrutinized concerning both SARA methods ASTM D 4124, and IFP 9305 applied to H-Oil VTBs, no such similarity as that observed for the SRVRs can be seen. This confirms the suggestion made above that the difference in the contents of SARA fractions reported by the various SARA methods can be diverse for distinct samples.

In order to verify the generality of the dependence of saturate content on the density of straight run vacuum residues established in Equation (1), we employed data of saturate content and density of 143 straight run vacuum residues extracted from 20 different literature sources and discussed in our earlier research [38]. This data set includes different methods for SARA measurement of straight run vacuum residues. Figure 3 summarizes the relationship of saturate content to the density of 165 straight run vacuum residues (143 data points from ref. [38] and 22 new points from the SAR-AD method studied in this work) employing different SARA methods. It is evident from this data that the dispersion of SAR-AD data is lower than that of the literature data, following the relationship established by Equation (1). It is also evident from the data in Figure 3 that the points of the other SARA methods are well described by the new regression Equation (1), which is a good indicator of the generality of the dependence established by Equation (1). Concerning the uncertainty of measurement, the method ASTM D 2007 [22] applicable to heavy oils reports repeatability of 2.1 wt.%, and reproducibility of 4.0 wt.% for saturate content, and the LNB method reports repeatability of 1.8 wt.% [24], while the standard ASTM D 4124 [19] does not report data for repeatability and reproducibility. The data in Figure 3 indicate that for some literature data, the dispersion is relatively large, reaching a 15 wt.% difference between measured and estimated by Equation (1) saturates content. This may be ascribed to the method employed or to a possible incorrect reporting of saturate content. The question of incorrect reporting has already been discussed in our earlier research [38], showing that a deviation higher than 4 wt.% of the reported saturate content from the regression model may require repeating the SARA measurement. Based on the data in Figure 3, one may conclude that Equation (1) could be considered to possess some kind of generalization of the dependence of saturate content on the density of straight run vacuum residues.

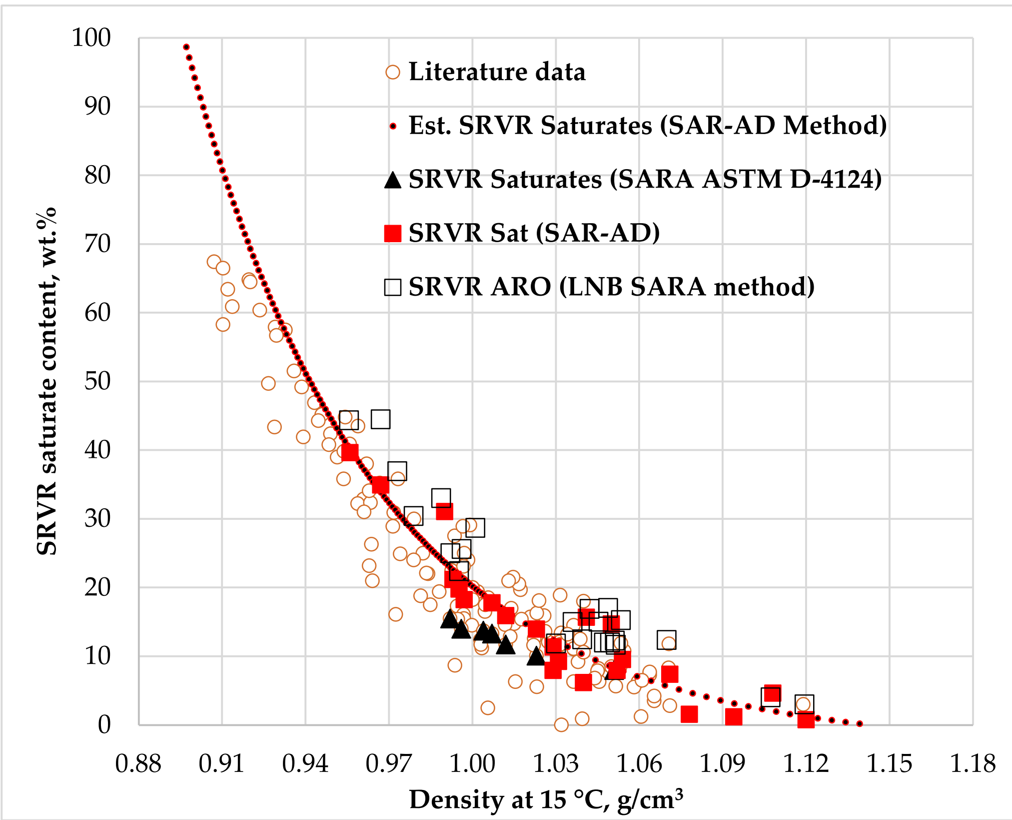

Figure 3. Dependence of saturate content on density of straight run vacuum residues (employing different SARA methods. (Red circle data was extracted from ref. [38]).

Similar regression dependencies of density of SRVRs, and H-Oil VTBs on the sum of contents of saturates and Aro-1 were developed, as shown in Equations (4) and (5).

$$\text{SRVR (Sat + Aro1)} = -220.7318 - \frac{100}{-0.4656+1600*\text{EXP}(-10.1565*D_{15})} \quad R = 0.95; \\ \text{av.dev.} = 3.1 \text{ wt.\%};\ \text{max. dev.} = 10.2 \text{ wt.\%};\ \text{bias} = -1.5 \text{ wt.\%} \tag{4}$$

$$\text{HOil VTB (Sat + Aro1)} = 240.7016 - \frac{100}{0.3769+6.7169*\text{EXP}(4.1432*D_{15})} \quad R = 0.98; \\ \text{av.dev.} = 0.84 \text{ wt.\%};\ \text{max. dev.} = 2.2 \text{ wt.\%};\ \text{bias} = -0.41 \text{ wt.\%} \tag{5}$$

Therefore, the density of the primary and secondary vacuum residues is an indicator for the contents of saturates for both LNB and SAR-AD^{TM} methods, and for saturates plus Aro-1 measured by the SAR-AD^{TM} method.

The data in Tables 6–9 indicate the presence of a statistically meaningful positive relation of the softening point of both SRVRs and H-Oil VTBs to SAR-AD^{TM} total asphaltene content for the SRVRs ($\mu = 0.87$; $\upsilon = 0.113$), and for H-Oil VTBs to SAR-AD^{TM} Aro-3 content ($\mu = 0.92$; $\upsilon = 0.08$). Using the computer algebra system Maple and NLPSolve with Modified Newton Iterative Method, the following models relating the softening point of SRVR and H-Oil VTB to the SRVR SAR-AD^{TM} total asphaltene content, and the H-Oil VTB SAR-AD^{TM} Aro-3 content were developed (Equations (6) and (7))

$$\text{SRVR (Total asp)} = 0.3255*SP_{SRVR} - 6.10 \quad R = 0.95; \\ \text{av.dev.} = 1.8 \text{ wt.\%};\ \text{max. dev.} = 6.4 \text{ wt.\%};\ \text{bias} = 0.3 \text{ wt.\%} \tag{6}$$

$$\text{HOil VTB Aro3} = 195.7533 - \frac{100}{28.0096-27.4617*\text{EXP}(-0.00009*SP_{HOIL\ VTB})} \quad R = 0.98; \\ \text{av.dev.} = 1.06 \text{ wt.\%};\ \text{max. dev.} = 2.6 \text{ wt.\%};\ \text{bias} = -0.10 \text{ wt.\%} \tag{7}$$

Figure 4 shows a graph of dependence of softening point on the SRVR SAR-AD^{TM} total asphaltene content, and on the H-Oil VTB SAR-AD^{TM} Aro-3 content.

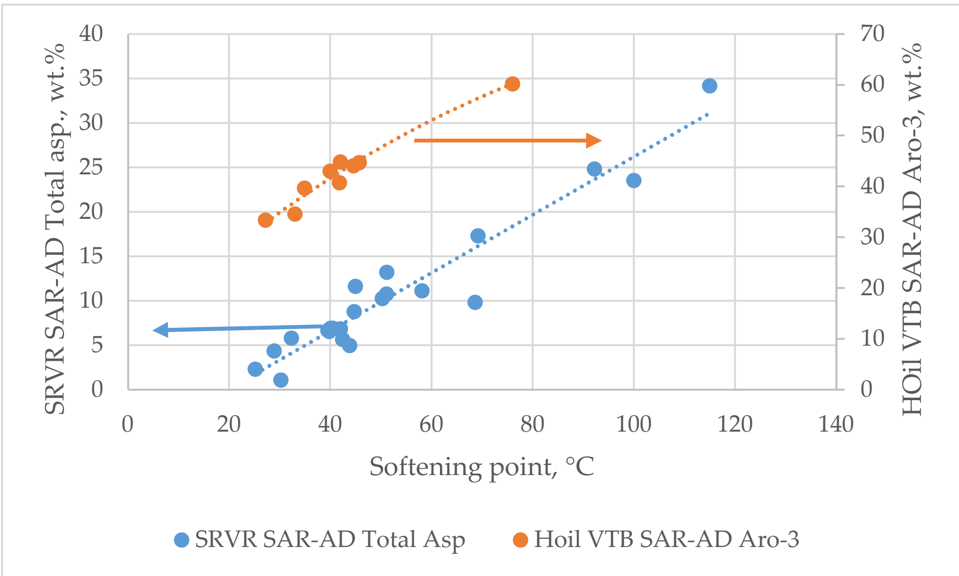

Figure 4. Dependence of softening point on the SRVR SAR-AD^{TM} total asphaltene content, and on the H-Oil VTB SAR-AD^{TM} Aro-3 content. (The orange arrow means that this data is referred to the right hand ordinate. The blue arrow implies that this data is referred to the left hand ordinate.)

These data suggest that the softening point of primary and secondary vacuum residues depends on structures containing 3:4 membered linear and catacondensed aromatics and large polycyclic aromatic hydrocarbons with a wide range of conjugation and connectivity (island or archipelago), including large molecules with molecular weights similar to asphaltenes [47]. The presence of such structures in SAR-AD™ Aro-3 fraction was identified by the use of model compounds, as reported in our earlier study [47]. These structures most probably are linked to each other in the SRVRs and fall in the asphaltene fraction, while in the H-Oil VTBs due to the high reaction temperature and long residence time in the H-Oil vacuum residue hydrocracking, the links between these structures are cracked and a smaller size of these structures, which cannot be distilled, and remain in the vacuum residue boiling range, fall in the Aro-3 fraction.

An interesting relation of SRVR SAR-AD™ cyclohexane soluble asphaltene content to the content of the fraction boiling above 540 °C (vacuum residue) was found by the intercriteria analysis evaluation (Tables 6 and 7) (μ = 0.88; υ = 0.091). This relation can be expressed by regression Equation (8).

$$\text{SRVR (CyC6 asp)} = 0.1465*X_{540^{\circ}+} - 1.37 \;\; R = 0.99;\ \text{av.dev.} = 0.26\ \text{wt.\%};\ \text{max. dev.} = 0.78\ \text{wt.\%};\ \text{bias} = 0.0\ \text{wt.\%} \quad (8)$$

This data suggests that the increase of vacuum residue fraction content in a crude oil is associated by increment of cyclohexane soluble asphaltene content. The data in Tables 6–9 indicate the presence of a very strong positive relation of total asphaltenes to toluene-soluble asphaltenes in both SRVRs, and H-Oil VTBs: (μ = 0.98; υ = 0.009) for SRVRs and (μ = 0.97; υ = 0.00). This relation is presented as a graph in Figure 5.

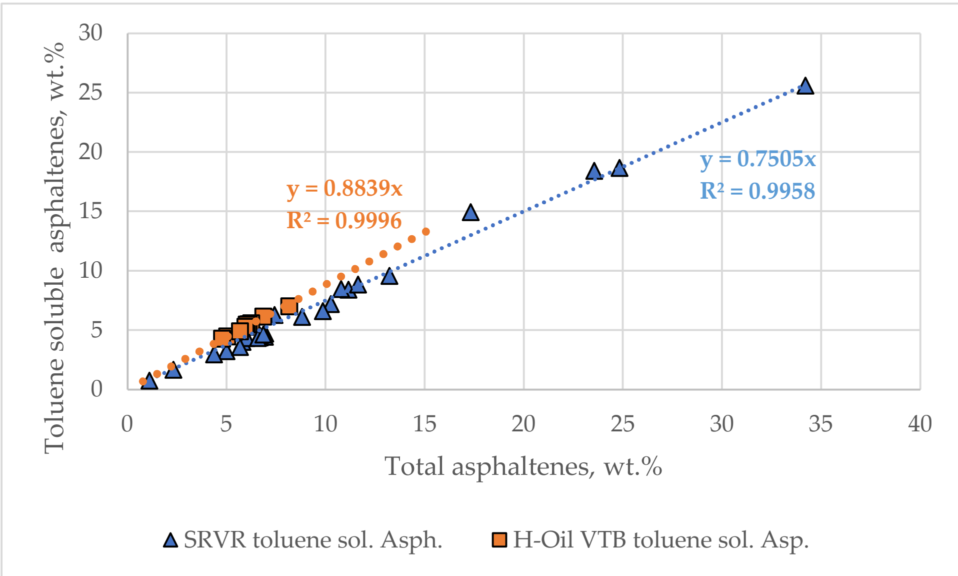

Figure 5. Relation of SAR-AD™ total asphaltene content to toluene-soluble asphaltene content.

The data in Figure 5 indicate that the predominant part of all asphaltenes in both SRVRs and H-Oil VTBs is toluene-soluble asphaltenes. It is interesting to note here that 75% of all asphaltenes in SRVRs are toluene soluble, while in the H-Oil VTBs, their part is bigger—88%. The data in Tables 6 and 7 show that the SRVR cyclohexane soluble asphaltene content has a positive statistically meaningful relation to the total asphaltene content measured by SAR-AD™ method (μ = 0.82; υ = 0.143). The H-Oil VTB cyclohexane soluble asphaltene content, however, exhibits dissonance with the total asphaltene content, as evident from the data in Tables 8 and 9 (μ = 0.58; υ = 0.39), implying no relation between them.

Figure 6 shows a graph of the relation of the cyclohexane soluble asphaltene content to the total asphaltene content measured by SAR-AD™ method. This data indicates that the SRVR cyclohexane soluble asphaltene content increases along with the total asphaltene content, and that the share of the cyclohexane soluble asphaltene is 22% of all asphaltenes.

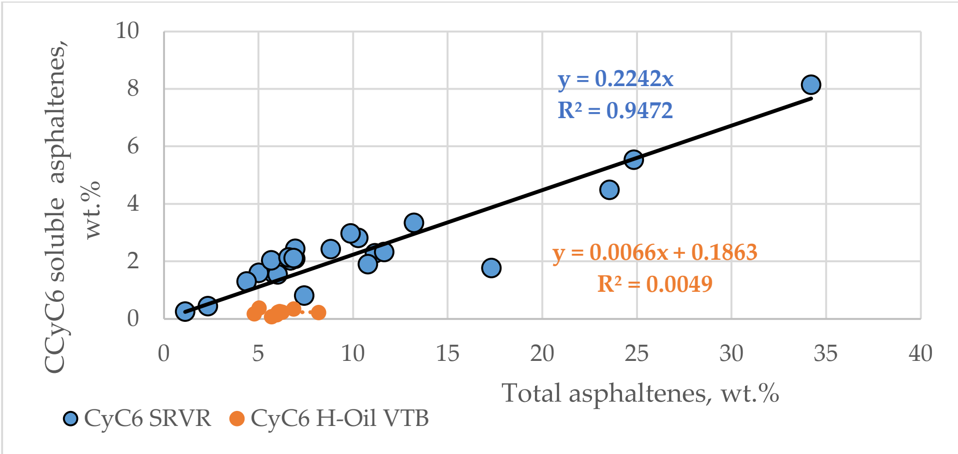

Figure 6. Relation of SAR-AD^{TM} total asphaltene content to cyclohexane-soluble asphaltene content.

The data in Tables 6 and 7 exhibit the presence of a weak statistically meaningful relation of SRVR SAR-AD^{TM} dichloromethane soluble asphaltene content to the total asphaltene content (μ = 0.74; υ = 0.095). The relation of H-Oil VTB dichloromethane soluble asphaltene content to the total asphaltene content, as evident from the data in Tables 8 and 9, is very weak (μ = 0.67; υ = 0.31). This is very well illustrated in the graph shown in Figure 7. The share of dichloromethane soluble asphaltene content is about 3% of all asphaltenes, and the squared correlation coefficient is much lower than that observed for the toluene soluble (Figure 5), and cyclohexane soluble (Figure 6) asphaltenes contents. The slope of dichloromethane-soluble asphaltene content increases with enhancement of the total asphaltene content in H-Oil VTB; however, it is three times as high as that of the SRVRs. This implies that in H-Oil vacuum residue hydrocracking, a redistribution in the asphaltene fractions occurs. It consists of a significant reduction of share of cyclohexane soluble asphaltenes (from 22% share in SRVR to about 3–4% share in H-Oil VTB), an increase of toluene soluble asphaltene share (from 75% to 88%), and an increase of share of dichloromethane soluble asphaltenes (from 2.6% to about 8%). This can explain the worsened colloidal stability of the H-Oil VTB relative to that of the SRVR.

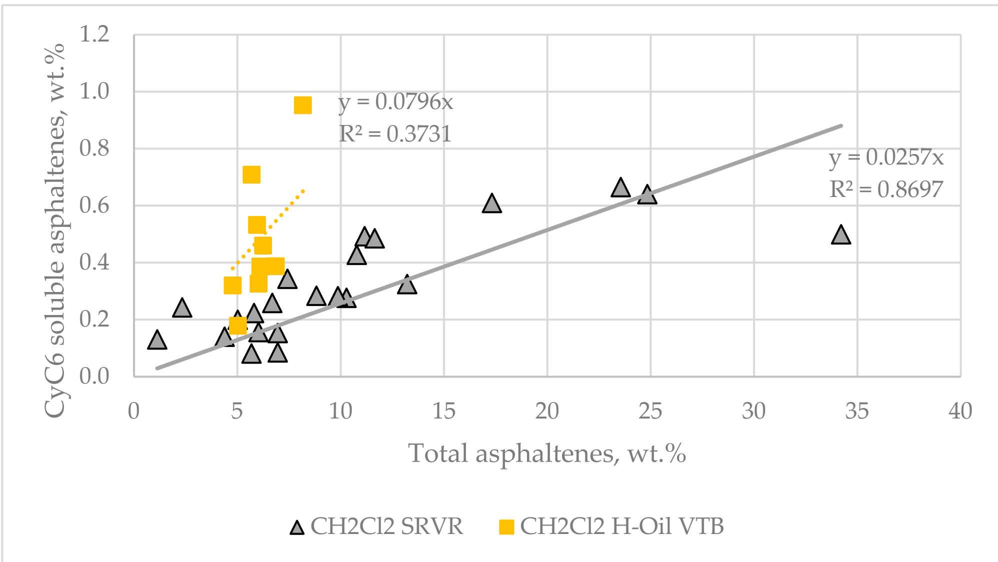

Figure 7. Relation of SAR-AD^{TM} total asphaltene content to dichloromethane-soluble asphaltene content.

The data in Tables 6 and 7 indicate the presence of a strong positive relation of LNB C_5-, and C_7-asphaltene content to the SAR-AD^{TM} total asphaltene content (μ = 0.92; υ = 0.074). Figure 8 illustrates the relation of the LNB C_7-asphaltene content to the SAR-AD^{TM} total asphaltene content. It is evident from this data that the SAR-AD^{TM} total asphaltene content is about 57% of the LNB asphaltene content. This finding is in line with our results reported in our earlier research showing that the SAR-AD^{TM} total asphaltene content is lower than the gravimetric heptane asphaltene content [47]. It is interesting to note the presence of outliers in the graph in Figure 6, that is, the asphaltene content from Boscan crude oil-derived vacuum residue. Both LNB method and the SAR-AD^{TM} method report almost the same value: about 34–35 wt.%. This observation suggests that, similar to the full SARA composition as discussed earlier in this study, the difference in asphaltene contents in the distinct vacuum residues seems to be sample specific.

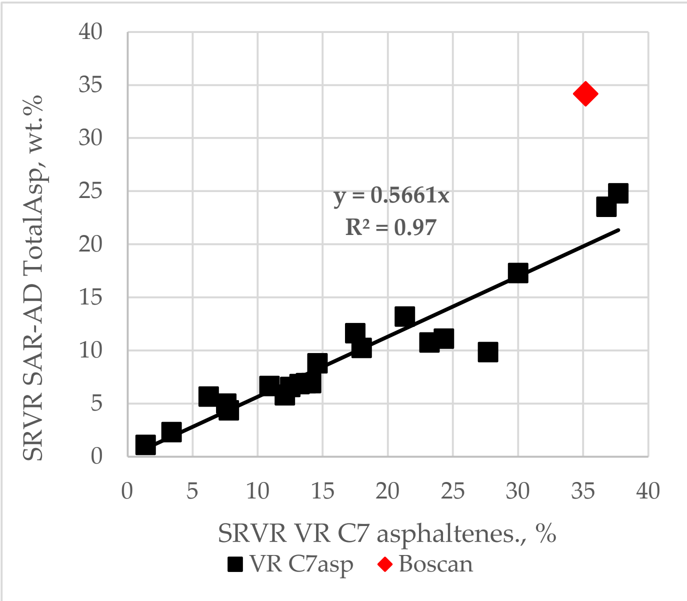

Figure 8. Relation of LNB C_7-asphaltene content to the SAR-AD^{TM} total asphaltene content.

In this research, we omitted discussing the relations of LNB SARA composition to vacuum residue bulk properties, which were already discussed in our earlier studies [38,40].

The intercriteria analysis allowed us to identify the relations between eight fractions SAR-AD^{TM} composition of SRVRs, and H-Oil VTBs to the vacuum residue bulk properties. It was found to be a helpful tool in determining statistically meaningful relations between different oil properties and oil refining process conditions. The statistically meaningful relations can be modeled by the use of the computer algebra system Maple and NLPSolve with the Modified Newton Iterative Method and regression equations obtained giving quantitative relations.

5. Conclusions

Intercriteria analysis evaluation was employed to determine the statistically meaningful relations of four fractions of LNB SARA composition data and eight fractions SAR-AD^{TM} composition data with bulk properties of twenty-two straight run vacuum residues extracted from extra light, light, medium, heavy, and extra heavy crude oils and nine different hydrocracked vacuum residues. It was found that the saturate content measured by both LNB and SAR-AD^{TM} methods can be predicted from the density of both straight run and hydrocracked vacuum residues. It was indicated that the new regression Equation (1) developed in this work possesses some kind of generalization and could be used as a tool to verify the correctness of the performed SARA measurement of straight run vacuum residues. The vacuum residue density was also found to be capable of predicting the sum of SAR-AD^{TM} fractions: saturates and Aro-1. The softening point of straight run vacuum residues was found to be capable of predicting the SAR-AD^{TM} total asphaltene fraction. The softening point of H-Oil hydrocracked vacuum residues was found to be capable of predicting the SAR-AD^{TM} Aro-3 fraction content.

The three SAR-AD^{TM} asphaltene fractions, cyclohexane soluble, toluene soluble, and dichloromethane soluble, were found to correlate with the SAR-AD^{TM} total asphaltene content for the straight run vacuum residues. The hydrocracked vacuum residue toluene soluble fraction content was the only SAR-AD^{TM} asphaltene fraction correlating with the SAR-AD^{TM} total asphaltene content. It was found that in hydrocracked vacuum residue hydrocracking, a redistribution in the asphaltene fractions occurs. It consists of a significant reduction of share of cyclohexane soluble asphaltenes (from 22% share in SRVR to about 3–4% share in H-Oil VTB), an increase of toluene soluble asphaltene share (from 75% to 88%), and an increase of share of dichloromethane soluble asphaltenes (from 2.6% to about 8%).

The SAR-AD^{TM} total asphaltene content was found to be equal to 56% of the LNB C_7-asphaltene content for all studied straight run vacuum residues except that of Boscan crude oil.

It was revealed that the difference in the contents of SARA fractions reported by the various SARA methods can be diverse for the distinct samples and seems to be sample specific.

It was proved again that intercriteria analysis is a useful tool to determine the statistically meaningful relations in complex oil systems that can be further modeled by the use of regression techniques. In the future, a study will be performed to contrast the four correlation analyses to the intercriteria analysis applied in the investigation of petroleum chemistry and processing.

Author Contributions: Conceptualization, D.S. and I.S.; methodology, D.S. and I.S.; software, S.N., S.R. and G.N.P.; validation, S.R. and D.N.; formal analysis, S.N. and G.N.P.; investigation, V.I.; resources, K.A.; data curation, G.N.P.; writing—original draft preparation, D.S. and I.S.; visualization, D.N.; supervision, K.A.; project administration, K.A.; funding acquisition, K.A. All authors have read and agreed to the published version of the manuscript.

Funding: This research was funded by the Bulgarian National Science Fund under Grant Ref. No. KP-06-N22-1/2018 "Theoretical research and applications of InterCriteria Analysis".

Data Availability Statement: Not applicable.

Acknowledgments: The authors would like to thank Jeramie J. Adams, Joseph F. Rovani, and Jean-Pascal Planche from the Western Research Institute for measurements of SAR-AD^{TM} compositions of the straight run and hydrocracked vacuum residues investigated in this study.

Conflicts of Interest: The authors declare no conflict of interest.

Nomenclature

Aro	Aromatic fraction content: wt.%
Asp	Asphaltenes content, wt.%
ATB	Atmospheric tower bottom product
av. dev.	Average deviation
CCR	Conradson carbon residue, wt.%
CH2Cl2	Dichloromethane
Conv.	Conversion, wt.%
CyC6	Cyclohexane
D_{15}	Density at 15 °C, g/cm^3
FBP	Final boiling point, °C
FCC	Fluid catalytic cracking
FID	Flame ionization detector
HCO	Heavy cycle oil
HPLC	High performance liquid chromatography

HTSD	High temperature simulated distillation
IBP	Initial boiling point, °C
ICrA	Intercriteria analysis
LNB	LUKOIL Neftohim Burgas
max.dev.	Maximum deviation
S	Sulphur content, wt.%
Sat	Saturates content, wt.%
SARA	Saturates, aromatics, resins, asphaltenes
SG	Specific gravity
SLO	Slurry oil from fluid catalytic cracking
SP	Softening point, °C
SRVR	Straight run vacuum residue
T_{50}	Temperature of 50% evaporate, °C
TBP	True boiling point
TLC	Thin layer chromatography
TRX	Reactor temperature, °C
TSE	Total sediment existent, wt.%
VTB	Vacuum tower bottom product
KV	Kinematic viscosity, cSt
VR	Vacuum residue
WABT	Weight average bed temperature, °C
WRI	Western Research Institute
X_{540+}	Weight percent of fraction boiling above 540 °C, %
μ	Positive consonance
υ	Negative consonance

References

1. Boduszynski, M.M. Composition of heavy petroleums. 2. Molecular characterization. *Energy Fuels* **1988**, *2*, 597–613. [CrossRef]
2. Altgelt, K.; Boduszynski, M. *Composition and Analysis of Heavy Petroleum Fractions*, 1st ed.; CRC Press: Boca Raton, FL, USA, 2014. [CrossRef]
3. Redelius, P.; Soenen, H. Relation between bitumen chemistry and performance. *Fuel* **2015**, *140*, 34–43. [CrossRef]
4. Corbett, L.W. Composition of asphalt based on generic fractionation, using solvent deasphaltening, elution-adsorption chromatography, and densimetric characterization. *Anal. Chem.* **1969**, *41*, 576–579. [CrossRef]
5. Stratiev, D.; Shishkova, I.; Kolev, I.; Yordanov, D.; Toteva, V. Petroleum crude slate effect on H-Oil performance. *Int. J. Oil Gas Coal Technol.* **2021**, *28*, 3. [CrossRef]
6. Hao, J.; Che, Y.; Tian, Y.; Li, D.; Zhang, J.; Qiao, Y. Thermal cracking characteristics and kinetics of oil sand bitumen and its SARA fractions by TG−FTIR. *Energy Fuels* **2017**, *31*, 1295–1309. [CrossRef]
7. Félix, G.; Ancheyta, J. Comparison of hydrocracking kinetic models based on SARA fractions obtained in slurry-phase reactor. *Fuel* **2019**, *241*, 495–505. [CrossRef]
8. Hauser, A.; Alhumaidan, F.; Al-Rabiah, H.; Absi Halabi, M. Study on thermal cracking of Kuwaiti heavy oil (vacuum residue) and its SARA fractions by NMR spectroscopy. *Energy Fuels* **2014**, *28*, 4321–4332. [CrossRef]
9. Xu, C.; Gao, J.; Zhao, S.; Lin, S. Correlation between feedstock SARA components and FCC product yields. *Fuel* **2005**, *84*, 669–674. [CrossRef]
10. Sinnathambi, C.M.; Mohamad-Nor, N. Relationship between SARA fractions and crude oil fouling. *J. Appl. Sci.* **2012**, *12*, 2479–2483. [CrossRef]
11. Fals, J.; Rafael-García, J.; Falco, M.; Sedran, U. Coke from SARA fractions in VGO. Impact on Y zeolite acidity and physical properties. *Fuel* **2018**, *225*, 26–34. [CrossRef]
12. Yarranton, H.W. Estimation of SARA fraction properties with the SRK EOS. *J. Can. Pet. Technol.* **2004**, *43*, 9. [CrossRef]
13. Farmani, Z.; Schrader, W. A Detailed look at the saturate fractions of different crude oils using direct analysis by ultrahigh resolution mass spectrometry (UHRMS). *Energies* **2019**, *12*, 3455. [CrossRef]
14. Guilhem, C.; Lienemann, C.P.; Merdrignac, I.; Bouyssiere, B.; Lobinski, R. Element speciation analysis of petroleum and related materials. *J. Anal. At. Spectrom.* **2009**, *24*, 263–276. [CrossRef]
15. Karevan, A.; Zirrahi, M.; Hassanzadeh, H. Standardized High-performance liquid chromatography to replace conventional methods for determination of saturate, aromatic, resin, and asphaltene (SARA) fractions. *ACS Omega* **2022**, *7*, 18897–18903. [CrossRef] [PubMed]
16. Keshmirizadeh, E.; Shobeirian, S.; Memariani, M. Determination of saturates, aromatics, resins and asphaltenes (SARA) fractions in Iran crude oil sample with chromatography methods: Study of the geochemical parameters. *J. Appl. Chem. Res.* **2013**, *7*, 15–24.
17. Jiang, C.; Larter, S.R.; Noke, K.J.; Snowdon, L.R. TLC—FID (Iatroscan) analysis of heavy oil and tar sand samples. *Org. Geochem.* **2008**, *39*, 1210–1214. [CrossRef]

18. Bissada, K.K.A.; Tan, J.; Szymczyk, E.; Darnell, M.; Mei, M. Group-type characterization of crude oil and bitumen. Part I: Enhanced separation and quantification of saturates, aromatics, resins and asphaltenes (SARA). *Org. Geochem.* **2016**, *95*, 21–28. [CrossRef]
19. *ASTM D4124-09*; Standard Test Methods for Separation of Asphalt into Four Fractions. American Society for Testing and Materials: West Conshohocken, PA, USA, 2012; Volume 403.
20. Rezaee, S.; Tavakkoli, M.; Doherty, R.; Vargas, F.M. A new experimental method for a fast and reliable quantification of saturates, aromatics, resins, and asphaltenes in crude oils. *Pet. Sci. Technol.* **2020**, *38*, 955–961. [CrossRef]
21. Karevan, A.; Yamchi, H.S.; Aghajamali, M.; Zirrahi, M.; Hassanzadeh, H. Automated high-performance liquid chromatography for SARA analysis (SARA-HPLC). *Energy Fuels* **2021**, *35*, 17642–17650. [CrossRef]
22. *ASTM D2007*; Standard Test Method for Characteristic Groups in Rubber Extender and Processing Oils and Other Petroleum–Derived Oils by the Clay–Gel Absorption Chromatographic Method. American Society for Testing and Materials: West Conshohocken, PA, USA, 2007.
23. Wu, W.; Saidian, M.; Gaur, S.; Prasad, M. Errors and repeatability in VSARA analysis of heavy oils. In Proceedings of the SPE Heavy Oil Conference Canada, Calgary, AB, Canada, 12–14 June 2012. [CrossRef]
24. Stratiev, D.; Shishkova, I.; Nikolova, R.; Tsaneva, T.; Mitkova, M.; Yordanov, D. Investigation on precision of determination of SARA analysis of vacuum residual oils from different origin. *Pet. Coal* **2016**, *58*, 109–119.
25. Adams, J.J.; Schabron, J.F.; Boysen, R. Quantitative vacuum distillation of crude oils to give residues amenable to the asphaltene determinator coupled with saturates, aromatics, and resins separation characterization. *Energy Fuels* **2015**, *29*, 2774–2784. [CrossRef]
26. Todorova-Yankova, L.; Yordanov, D.; Stratiev, D.; Shishkova, I. Investigation of the group hydrocarbon composition of vacuum residues from different types of crude oil, crude oil sands and bitumens. *Ind. Technol.* **2021**, *8*, 51–64. (In Bulgarian)
27. Zhang, J.; Tian, Y.; Qiao, Y.; Yang, C.; Shan, H. Structure and reactivity of Iranian vacuum residue and its eight group-fractions. *Energy Fuels* **2017**, *31*, 8072–8086. [CrossRef]
28. Rudyk, S. Relationships between SARA fractions of conventional oil, heavy oil, natural bitumen and residues. *Fuel* **2018**, *216*, 330–340. [CrossRef]
29. Fan, T.; Wang, J.; Buckley, J.S. Evaluating Crude oils by SARA analysis. In Proceedings of the SPE/DOE Improved Oil Recovery Symposium, Tulsa, OK, USA, 13–17 April 2002. SPE-75228-MS. [CrossRef]
30. León, A.Y.; Parra, M.; Grosso, J.L. Estimation of critical properties of typically Colombian vacuum residue SARA fractions. *CTF-Cienc. Tecnol. Futuro* **2008**, *3*, 129–142. [CrossRef]
31. Che, Y.; Yang, Z.; Qiao, Y.; Zhang, J.; Tian, Y. Study on pyrolysis characteristics and kinetics of vacuum residue and its eight group-fractions by TG-FTIR. *Thermochim. Acta* **2018**, *669*, 149–155. [CrossRef]
32. Zhang, J.; Niwamanya, N.; Gao, C.; Sekyere, D.T.; Barigye, A.; Tian, Y. Structure and millisecond pyrolysis behavior of heavy oil and its eight group-fractions on solid base catalyst. *Fuel* **2022**, *318*, 123483. [CrossRef]
33. Meléndez, L.V.; Lache, A.; Orrego-Ruiz, J.A.; Pachón, Z.; Mejía-Ospino, E. Prediction of the SARA analysis of Colombian crude oils using ATR–FTIR spectroscopy and chemometric methods. *J. Pet. Sci. Eng.* **2012**, *90–91*, 56–60. [CrossRef]
34. Reyes-Gonzalez, D.; Ramirez-Jaramillo, E.; Manero, O.; Lira-Galeana, C.; del Rio, J.M. Estimation of the SARA Composition of Crude Oils from Bubblepoint Pressure Data. *Energy Fuels* **2016**, *30*, 6913–6922. [CrossRef]
35. Yarranton, H. Prediction of Crude Oil Saturate Content from a SimDist Assay. *Energy Fuels* **2022**, *36*, 8809–8817. [CrossRef]
36. Sanchez-Minero, F.; Ancheyta, J.; Silva-Oliver, G.; Flores-Valle, S. Predicting SARA composition of crude oil by means of NMR. *Fuel* **2013**, *110*, 318–321. [CrossRef]
37. Stratiev, D.; Shishkova, I.; Tsaneva, T.; Mitkova, M.; Yordanov, D. Investigation of relations between properties of vacuum residual oils from different origin, and of their deasphalted and asphaltene fractions. *Fuel* **2016**, *170*, 115–129. [CrossRef]
38. Stratiev, D.; Nenov, S.; Shishkova, I.; Georgiev, B.; Argirov, G.; Dinkov, R.; Yordanov, D.; Atanassova, V.; Vassilev, P.; Atanassov, K. Commercial investigation of the ebullated-bed vacuum residue hydrocracking in the conversion range of 55–93%. *ACS Omega* **2020**, *51*, 33290–33304. [CrossRef] [PubMed]
39. Stratiev, D.; Shishkova, I.; Nikolaychuk, E.; Atanassova, V.; Atanassov, K. Investigation of relations of properties of straight run and H-Oil unconverted vacuum residual oils. *Pet. Coal* **2019**, *61*, 763–776.
40. Stratiev, D.; Shishkova, I.; Dinkov, R.; Kolev, I.; Argirov, G.; Ivanov, V.; Ribagin, S.; Atanassova, V.; Atanassov, K.; Stratiev, D.D.; et al. Intercriteria analysis to diagnose the reasons for increased fouling in a commercial ebullated bed vacuum residue hydrocracker. *ACS Omega* **2022**, *7*, 30462–30476. [CrossRef] [PubMed]
41. *ASTM D4052-22*; Standard Test Method for Density, Relative Density, and API Gravity of Liquids by Digital Density Meter. American Society for Testing and Materials: West Conshohocken, PA, USA, 1996.
42. *ASTM D4294-21*; Standard Test Method for Sulfur in Petroleum and Petroleum Products by Energy Dispersive X-ray Fluorescence Spectrometry. American Society for Testing and Materials: West Conshohocken, PA, USA, 2010.
43. *ASTM D2892-20*; Standard Test Method for Distillation of Crude Petroleum (15-Theoretical Plate Column). American Society for Testing and Materials: West Conshohocken, PA, USA, 2010.
44. *IFP 9305*; Petroleum Products Separation of Saturates, Aromatics, Resins and Asphaltenes fractions Liquid Adsorption Chromatography. IFP (French Insitute of Petroleum): Rueil-Malmaison, France.

45. Boysen, R.B.; Schabron, J.F. The automated asphaltene determinator coupled with saturates, aromatics, and resins separation for petroleum residua characterization. *Energy Fuels* **2013**, *27*, 4654–4661. [CrossRef]
46. Adams, J.; Elwardany, M.; Planche, J.; Boysen, R.; Rovani, J. Diagnostic techniques for various asphalt refining and modification methods. *Energy Fuels* **2019**, *33*, 2680–2698. [CrossRef]
47. Adams, J.J.; Rovani, J.F.; Planche, J.-P.; Stratiev, D.; Shishkova, I.; Kolev, I.; Atanassov, K.; Nenov, S.; Ribagin, S.; Stratiev, D.; et al. SAR-AD Method to Characterize Vacuum Residues from Different Origins as a Tool to Investigate the Performance of a Commercial Ebullated Bed Vacuum Residue Hydrocracker. Available online: https://papers.ssrn.com/sol3/papers.cfm?abstract_id=4252478 (accessed on 24 November 2022).
48. Diarov, I.N.; Batueva, I.U.; Sadikov, A.N.; Colodova, N.L. *Chemistry of Crude Oil*; Chimia Publishers: St. Peterburg, Russia, 1990. (In Russian)